PHYSICAL REVIEW E **67**, 060103(R) (2003)

Anomalous growth of the depletion zone in the photobleaching trapping reaction

Sung Hyun Park, Hailin Peng, and Raoul Kopelman
Department of Chemistry, University of Michigan, Ann Arbor, Michigan 48109-1055, USA

Panos Argyrakis
Department of Physics, University of Thessaloniki, Thessaloniki 54124, Greece

Haim Taitelbaum
Department of Physics, Bar-Ilan University, Ramat-Gan 52900, Israel
(Received 20 February 2003; published 20 June 2003)

We study the anomalous growth of the depletion zone at a single trap, as observed in a photobleaching trapping reaction in confined geometry. We provide experimental evidence for a nonuniversal growth of this depletion. We also find an early-time behavior of the depletion zone, owing to the finite size of the trap. Various laser powers are used in order to study the effects of trapping strength, interpreted theoretically in terms of an imperfect trap. The results are supported by numerical calculations. Comparison with other trapping reactions provides insight into finite-size traps.

DOI: 10.1103/PhysRevE.67.060103 PACS number(s): 82.50.−m

The trapping reaction is the simplest chemical reaction and is a model for a variety of transport processes [1]. It can be formulated as $A+B\rightarrow B$, where A is a particle and B is a trap. This corresponds to the original Smoluchowski work on coagulation [2], a process involving the trapping of mobile particles A by stationary aggregates B, which became the basis for classical reaction theory. It has become evident that in low dimensions the kinetic properties can differ significantly from classical results, and that these anomalous reaction-diffusion laws are related to the self-organization of the reactants. A number of recent papers [3–11] have been devoted to the problem of depletion zones in the vicinity of a single trap. A possible measure of this depletion is the distance from the trap to a point where the concentration of A's is equal to a given arbitrary fraction θ $(0<\theta<1)$, of its bulk value, hereafter referred to as the θ distance. This is given by

$$p(r_\theta,t)=\theta c_0, \tag{1}$$

where $p(r,t)$ is the concentration profile of A particles at distance r at time t, starting from an initial constant concentration c_0 at time $t=0$.

In one dimension, the θ distance has been shown, theoretically [3,4] and experimentally [11] to increase asymptotically like $t^{1/2}$. In three dimensions, the depletion zone is localized and the θ distance is time independent.

The two-dimensional case is the most interesting one [8–10]. For a trap having a circular, disklike shape, the concentration profile in the neighborhood of the trap has been found to grow like $(\ln r/\ln t)$, yielding a $t^{\theta/2}$ nonuniversal scaling for the θ distance. The trap absorptivity, ranging between perfect trapping and total reflection, can be described in terms of the radiation boundary condition [12]. Exact expressions have been derived for the concentration profiles in the vicinity of a two-dimensional trap, as well as for the θ distance in the long-time limit [10].

However, no experimental confirmation of these anomalous results in low dimensions has been reported. In this paper, we report on an experimental setup for measuring the θ distance in low dimensions. The experiment is the photobleaching of fluorescein dye molecules by a focused laser beam in a very shallow trough (150-μm-thin cell). This ''phototrap'' system is directly relevant to the reaction dynamics for intracellular optochemical nanosensors as well as for photodynamic nanoexplorers [13,14]. In general, phototraps play an important role in various dynamical processes, ranging from atmospheric ozone depletion to photodynamic cancer therapy. They are at the focus of photophysics and are highly important to novel photoresist nanotechnology [15].

In our experiment, the laser beam is focused into a cylindrical shape to produce an effectively two-dimensional environment with a circular trap cross section on the sample plane (Fig. 1). Two different laser powers were used to examine the effect of the trap strength, one at 12 mW from a 488-nm beam out of an air-cooled Ar-ion laser and the other at 130 mW from femtosecond pulse at 430 nm out of a frequency doubler coupled with a Ti:sapphire laser. Another light source at 480 ± 5 nm, with ≈1 in diameter from a mercury lamp illuminated from below, was used to probe the

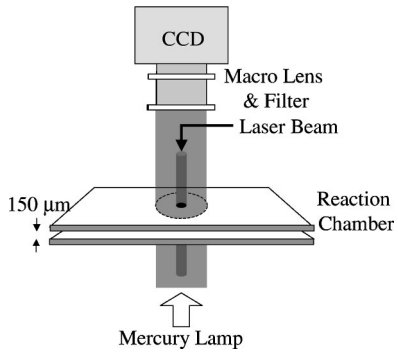

FIG. 1. A schematic diagram of the experimental setup.

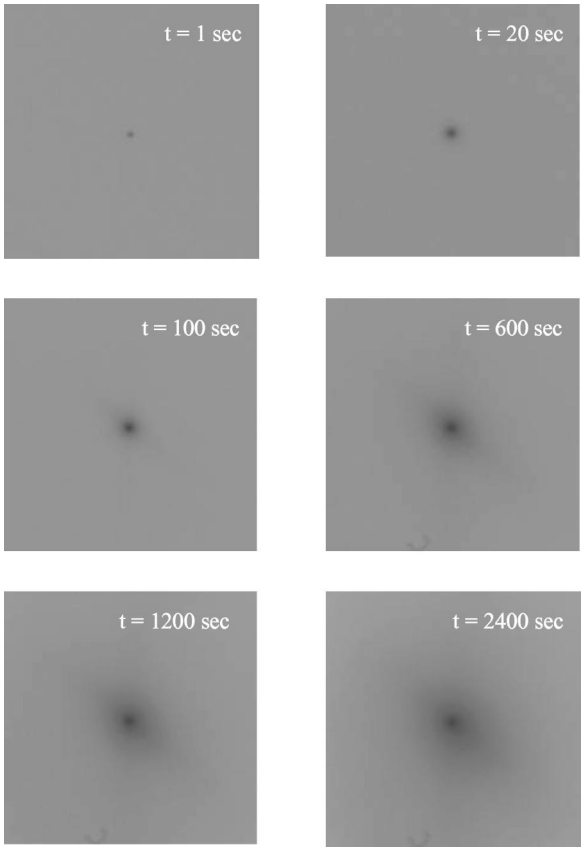

FIG. 2. A series of fluorescence images of the fluorescein molecules around the trap at $t=1$, 20, 100, 600, 1200, and 2400 s of photobleaching. Dark regions in the center show the growth in time of the depletion zone around the phototrap.

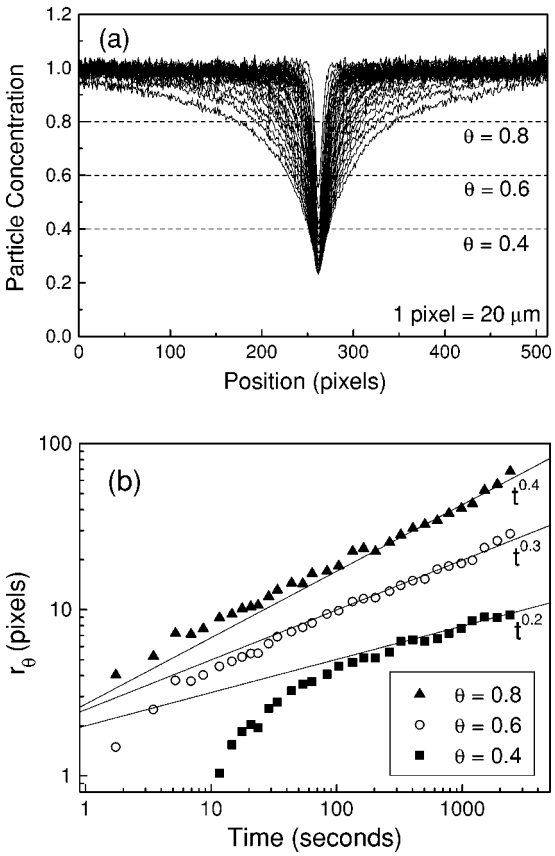

FIG. 3. (a) Typical temporal evolution of the spatial concentration profiles of the fluorescein along an arbitrary pixel line through the center of the trap, at times ranging from 1.7 s up to about 40 min. The laser power is 12 mW and each pixel is 20 μm. Dotted horizontal lines at the chosen values of $\theta=0.4$, 0.6, 0.8 are plotted for measuring θ distances; (b) a plot of the θ distance vs time for the experimental data shown in (a), for the chosen values of θ. The θ distances, growing as $t^{\theta/2}$ asymptotically, show nonuniversal behaviors. At short times and near the center of the trap, the θ distances grow at a much faster rate.

progress of the photobleaching reaction. The images of fluorescence emission from the sample were collected at different times, using a charge-coupled device (CCD) camera, equipped with a macrolens. A series of CCD snapshots are shown in Fig. 2. The scale of the image is 1×1 cm^2 with a 512×512 resolution. The dye molecule becomes invisible from the detector when photobleached, resulting in an intensity drop in the fluorescence image. The dark region in the center of the images in Fig. 2, hence, represents the growth of the depletion zone around the trap. Further technical details can be found in Ref. [11]. This experimental design allows one to measure the temporal changes in the spatial distribution of reactants at the trap and to obtain the θ distance.

Figure 3(a) shows typical temporal evolutions of the spatial concentration profiles along one arbitrary pixel line through the center of the trap. The corresponding plots of the behavior of θ distance as a function of time are shown in Fig. 3(b), for the values of θ chosen in Fig. 3(a).

The curves in Fig. 3(b) provide the experimental evidence for the nonuniversal growth of the θ distance, $t^{\theta/2}$, which depends on the arbitrary chosen parameter θ. This is due to the logarithmic form of the two-dimensional profile. Moreover, it can be seen that, for short times and close to the origin, the θ distance grows at a much faster rate, prior to the convergence to the asymptotic (and nonuniversal) slope. This result has been reproduced in a set of numerical simulations using various techniques, which will be published elsewhere.

A closer look at the concentration profiles at the vicinity of the trap allows one to interpret this early-time–short-distance regime. From Fig. 4, it is evident that the profile changes its curvature at the disk-trap boundary. The positive slope outside the disk changes to an eventual zero slope at the center of the trap. This observation can be explained on the basis of the following theoretical arguments.

Let the trap be a circle of radius a. Mobile A particles are assumed to be initially uniformly distributed throughout the entire plane with concentration c_0. The solution of the diffusion equation governing the diffusion of A particles in the infinite two-dimensional region bounded internally by the circle $r=a$ (i.e., *outside* the trap), subject to the radiation boundary condition,

$$\left.\frac{\partial p}{\partial r}\right|_{r=a} = \kappa p|_{r=a}, \tag{2}$$

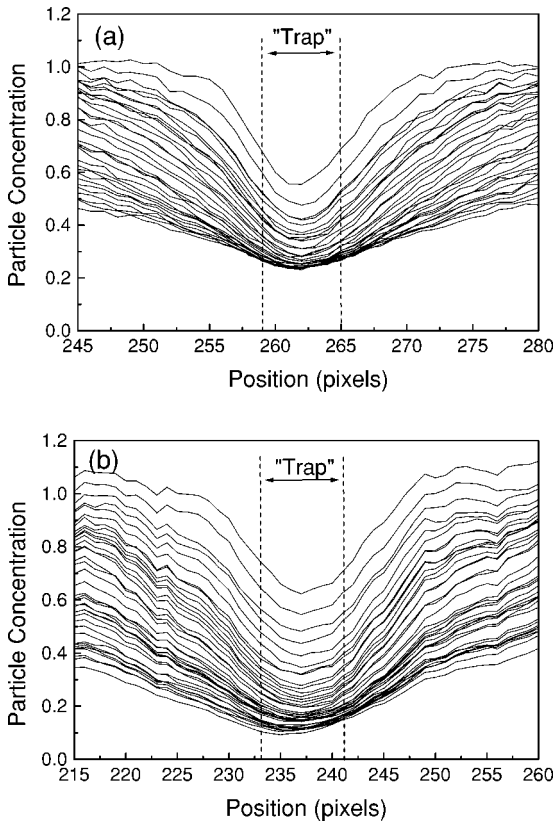

FIG. 4. (a) The experimental concentration profiles at the vicinity of the trap, taken from Fig. 3(a). Laser power is 12 mW. The diameter of the disk trap, shown by the vertical dotted lines, is ≈6 pixel long. Note the change of curvatures in profiles across the trap boundary; (b) similar to (a), but from an experiment with a stronger laser power of 130 mW.

has been shown in Ref. [10] to be given asymptotically by

$$p(r,t)\simeq 2c_0\left[\ln\left(\frac{r}{a}\right)+\frac{1}{\kappa a}\right]\left[\frac{1}{\ln(4T)-2\gamma+\frac{2}{\kappa a}}-\frac{\gamma}{\left[\ln(4T)-2\gamma+\frac{2}{\kappa a}\right]^2}+\cdots\right], \tag{3}$$

where $T\equiv Dt/a^2$ is a dimensionless time parameter, $\gamma=0.577\,22...$ is Euler's constant, and κ is a measure of the reaction strength at the interface $r=a$, ranging from $\kappa=\infty$ for a perfectly absorbing trap, down to $\kappa=0$ for total reflection (no reaction). From this follows the result for r_θ in the long-time limit [10],

$$r_\theta\simeq a(4T)^{\theta/2}\exp\left\{-\frac{1}{\kappa a}(1-\theta)\right\}. \tag{4}$$

This result, shown also in Fig. 5, is valid outside the trap. An analytical solution for the concentration profile of diffusing particles *inside* a finite trapping region is not available. However, it is physically plausible that the profile inside the finite trap can be approximated by a relatively flat curve for any given time. This is due to the uniform concentration c_0 of particles in this region prior to the beginning of the photobleaching trapping reaction. This argument is supported by solutions for a related problem of a ringlike trap (i.e., trapping only at the boundary $r=a$) [12]. Next, in order to match these outside and inside profiles at the trap boundary, the profile curve must change its curvature. The concave shape inside the trap explains the early-time–short-distance increase of the θ distance, which is just the distance to this curve. Outside the trap, the profile is convex, which gives rise to slower increase of the distance in this curve. Thus, the combined shape of the profile explains the two regions found for the behavior of the θ distance.

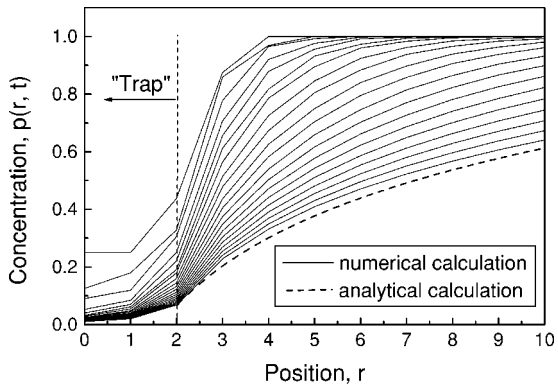

FIG. 5. The reactant concentration profiles at different times (2 up to 10^3) from numerical calculations using recursion formula for a finite-size imperfect trap in two dimensions. The trap is a 13-point diamond shape on a square lattice, with a constant trapping probability, $p=0.5$, at all of its 13 points. Dotted lines represent the analytical result [Eq. (3)] *outside* the finite trap, with $\kappa=6$, $a=2$, and $T=18.5$.

In Fig. 5, we plot results from an exact enumeration calculation on a two-dimensional square lattice, where an imperfect trap with a finite radius of two lattice sites and with a finite trapping probability ($p=0.5$ in the figure) is located in its origin. The results are in excellent agreement with the experimental data, and support the above argumentation. Dotted lines are obtained from Eq. (3) for the profile outside the trap perimeter.

It can be seen in Figs. 4(a),4(b) that as time increases, the value of the profile at the center of the trap, $p(0,t)$, tends to converge to an approximately constant value. In fact, from Eq. (3), valid for $r\geqslant a$, this value decays asymptotically as $(\ln t)^{-1}$ at the boundary of the disk ($r=a$). Since the profile inside the trap is approximately flat, this slow logarithmic decay of $p(a,t)$ yields, in fact, an approximation for a lower bound for the entire profile, hence a lower bound for the arbitrary choice of the parameter θ. Lower values for the arbitrary θ are simply not possible.

Moreover, the value of the profile of the diffusion particles at the bottom of the profile curve depends only on the trapping efficiency κ. This enables one to obtain an explicit relation between the laser power and the theoretical trapping strength. For example, in Fig. 4(a), for laser power of 12

mW, the low value of the profile is around 0.25, while for higher laser power (130 mW), shown in Fig. 4(b), the value is close to 0.1. From Eq. (3), these values at the trapping boundaries correspond, roughly, to $\kappa \simeq 2$ and $\kappa \simeq 5$, respectively.

It is interesting to compare these results for a finite-sized trap to results obtained for a single *mobile* trap in one dimension [16–18]. The concentration profile of the diffusing particles (in the so-called laboratory coordinate system) has been shown to exhibit a flat, zero-slope, region at the origin, i.e., in the position of the trap at $t=0$. In light of our results for a finite-size trap, this flat profile in the center means that the moving point trap creates an *effective* finite-sized trapping region as time evolves. When the trap is static, or in the opposite case when the particles are static, the profile at the center has a positive slope, because in these two cases the effective trapping region is either a point or effectively infinite, respectively. It is only in the case when both the trap and the particles are mobile that an effective *finite* trapping region is formed and induces a flat profile at the center.

In summary, we have studied the properties of the depletion zone at a finite-size phototrap in two dimensions, by analyzing the concentration profile of the diffusing particles through the θ distance measure. Our experimental technique confirms the nonuniversality of this measure, as well as an early-time–short-distance behavior resulting from the finite disklike shape of the trap. Comparison with theoretical and numerical results allows one to attribute a trapping strength parameter to the laser power used in the photobleaching experiment. More insight into finite-sized traps is obtained by comparison to the shape of the concentration profile in the case of a *mobile* trap in one dimension.

Further issues to be addressed in the extended version of this paper are the effect of the exact distribution of the laser beam power throughout the disk trap, and also the effect of the disk width (i.e., possible crossover from two-dimensional to three-dimensional behavior).

Support by NSF Grant No. DMR9900434 is gratefully acknowledged.

[1] F. den Hollander and G. H. Weiss, in *Contemporary Problems in Statistical Physics*, edited by G. H. Weiss (SIAM, Philadelphia, 1994).
[2] M. V. Smoluchowski, Z. Physik. Chem. **92**, 129 (1917).
[3] G. H. Weiss, R. Kopelman, and S. Havlin, Phys. Rev. A **39**, 466 (1989).
[4] D. Ben-Avraham and G. H. Weiss, Phys. Rev. A **39**, 6436 (1989).
[5] H. Taitelbaum, R. Kopelman, G. H. Weiss, and S. Havlin, Phys. Rev. A **41**, 3116 (1990).
[6] H. Taitelbaum, S. Havlin, and G. H. Weiss, Chem. Phys. **146**, 351 (1990).
[7] R. Schoonover, D. Ben-Avraham, S. Havlin, R. Kopelman, and G. H. Weiss, Physica A **171**, 232 (1991).
[8] S. Havlin, H. Larralde, R. Kopelman, and G. H. Weiss, Physica A **169**, 337 (1990).
[9] S. Redner and D. Ben-Avraham, J. Phys. A **23**, L1169 (1990).
[10] H. Taitelbaum, Phys. Rev. A **43**, 6592 (1991).
[11] S. H. Park, H. Peng, S. Parus, H. Taitelbaum, and R. Kopelman, J. Phys. Chem. A **106**, 7586 (2002).
[12] H. S. Carslaw and J. C. Jeager, *Conduction of Heat in Solids*, 2nd ed. (Oxford University Press, Oxford, 1959), Chaps. 7 and 13.
[13] M. Brasuel, R. Kopelman, T. J. Miller, R. Tjalkens, and M. A. Philbert, Anal. Chem. **73**, 2221 (2001).
[14] E. Monson, M. Brasuel, M. A. Philbert, and R. Kopelman, *Biomedical Photonics Handbook* (CRC Press, Boca Raton, 2003), Chap. 59.
[15] E. K. Lin *et al.*, Science **297**, 372 (2002).
[16] Z. Koza and H. Taitelbaum, Phys. Rev. E **57**, 237 (1998).
[17] A. D. Sanchez, M. A. Rodriguez, and H. S. Wio, Phys. Rev. E **57**, 6390 (1998).
[18] A. D. Sanchez, Phys. Rev. E **59**, 5021 (1999).